Green Synthesis and Functionalization of Au Nanoparticles using Syzygium samarangense Leaf Extract and its Biological Applications

Chaudhary Leela*, Chaudhary Mansi, Patel Nidhi, Moga Himani and Makvana Chirag
Department of Chemistry, Gokul Global University, Sidhpur, Gujarat, 384151, INDIA
*chaudharyleela378@gmail.com

Abstract

Nanotechnology has revolutionized various industries with gold nanoparticles (AuNPs) being particularly significant due to their biocompatibility and versatile applications. Traditional synthesis methods for AuNPs often involve harsh chemicals, raising concerns about environmental sustainability. Using leaf extract from Syzygium samarangense as a reducing agent, this work investigates the green synthesis of AuNPs which provides a more environmentally friendly technique. The leaf extract's abundant phytoconstituents, such as phenolic acids and flavonoids, stabilize the nanoparticles in addition to lowering the gold ions.

To further improve these AuNPs' stability and biocompatibility, we functionalized them using polyvinyl pyrrolidone (PVP). The effective synthesis and functionalization of the produced PVP-b-AuNPs were confirmed by characterization utilizing FTIR, HR-TEM, XRD and UV-Vis spectroscopy. Biological evaluations revealed that PVP-b-AuNPs exhibit superior antioxidant and antimicrobial activities compared to unfunctionalized b-AuNPs. These findings highlight the potential of S. samarangense leaf extract in the sustainable synthesis of functionalized AuNPs, providing a scalable, eco-friendly alternative for applications in healthcare and other industries.

Keywords: *Syzygium samarangense*, Green synthesis, Gold nanoparticles, PVP functionalization, Biological activity.

Introduction

The development of nanotechnology has revolutionized a number of sectors such as electronics, healthcare and catalysis, by taking use of the special properties of materials with sizes ranging from one to one hundred nanometers[1]. AuNPs, in particular, have fascinated significant attention because of their exceptional biocompatibility, non-toxic nature and versatility in applications[2]. However, conventional methods of synthesizing AuNPs often involve the use of harsh chemicals and conditions which can compromise their environmental sustainability[3].

In response to this challenge, green synthesis techniques have emerged as a viable alternative, utilizing plant-based materials as reducing agents to produce AuNPs[4]. The tropical plant species *S. samarangense* has been shown to be a viable option for this use because of wide variety of phytoconstituents which include terpenoids, phenolic acids and flavonoids[1]. Since these substances have been demonstrated to have antibacterial, anti-inflammatory and antioxidant qualities, *S. samarangense* leaf extract is a perfect reducing agent for the production of AuNPs[5].

The synthesis of AuNPs using plant-based materials has several benefits such as affordability, scalability and environmental sustainability[6]. Additionally, the phytoconstituents present in *S. samarangense* leaf extract may impart unique properties to the synthesized AuNPs such as enhanced antioxidant activity[5]. The functionalization of AuNPs with PVP can further enhance their stability and biocompatibility[7]. PVP-b-AuNPs have been shown to exhibit improved antioxidant activity and antibacterial properties compared to unfunctionalized AuNPs[2].

Natural phytochemicals serve as stabilizing and reducing agents and recent research has demonstrated the efficiency of plant-based methods to develop stable and biocompatible gold nanoparticles. For instance, phytochemicals like flavonoids and phenolic acids not only reduce gold ions but also coat the nanoparticles, enhancing their stability and bioactivity[8]. This biogenic synthesis process leverages renewable plant materials, reducing the environmental footprint typically associated with nanomaterial production[9]. Furthermore, the use of plant extracts, such as *Syzygium samarangense* leaf extract, has been linked to unique nanoparticle properties, particularly due to the bioactive compounds that enhance antioxidant and antimicrobial activities[10].

Recent studies have provided more evidence that functionalizing AuNPs with polyvinyl pyrrolidone is a successful method for enhancing the stability, biocompatibility and effectiveness of nanoparticles for use in biomedical applications. Functionalized PVP-b-AuNPs show promising antimicrobial properties, with recent works reporting enhanced activity against drug-resistant bacterial strains. This synergy between plant-based synthesis and polymer functionalization expands the scope of AuNP applications, making them suitable for targeted therapeutic and diagnostic applications[11-16].

In line with these advancements, the current study aims to characterize PVP-functionalized AuNPs synthesized from *S. samarangense* using advanced analytical techniques including FTIR, UV-Vis spectroscopy, XRD and HR-TEM.This approach not only ensures sustainable production

but also enhances the biomedical potential of AuNPs, positioning them as viable candidates for next-generation antimicrobial agents and antioxidants.

Material and Methods

Material and Characterization Techniques: PVP with a molecular weight of 40,000 and $AuCl_4$ (gold chloride) were acquired from Sigma-Aldrich and ACS respectively. SRL India provided the butylated hydroxytoluene (BHT) and DPPH. The leaves of *S. samarangense* were gathered in Banaskantha, Gujarat, India's Deesa village. The antimicrobial pathogens were obtained from the Microbial Type Culture Collection (MTCC) located in Chandigarh, Punjab, India. Throughout, Milli-Q water, also known as ultrapure water, was utilized to produce the solutions. The UV spectrum was recorded using a Shimandu-1800 UV-Vis spectrophotometer. The XRD investigation was carried out using the Rigaku D/max 40 kV X-ray diffraction spectrometer. FTIR analysis was carried out on a FTIR spectrometer equipped with a KBr disc in the 400–4000 cm^{-1} range. The structural morphology was examined by HR-TEM.

Leaf Extract Preparation: Milli-Q water was used to clean 10 grams of fresh *S. samarangense* leaves in order to get rid of unwanted elements. After being thoroughly cleaned and dried using filter paper, *S. samarangense* leaves were pulverized using a grinder. Dried leaf powder was added to 100 cc of milli-Q water and heated to 40–50 °C while being stirred constantly for ten minutes. Whatmann filter paper was used to filter the leaf extract once it had cooled. The obtained yellowish-colored solution was kept for later use in a deep freezer at -10 °C (Fig. 1).

Synthesis of Gold Nanoparticles (b-AuNPs): A freshly made *S. samarangense* leaf extract (10 mL) and a 1 mM $AuCl_4$ solution (90 mL prepared in milli-Q water) were combined in a conical flask and for six hours, the mixture was heated to 60 °C while being constantly stirred. The yellowish liquid changed into a dark brown suspension after six hours. After cooling for 20 minutes, the mixture was centrifuged for around 20 minutes at 10,000 rpm and 20 °C. The obtained nanoparticles were dried at 70–75 °C for four hours after being cleaned with pure water (Fig. 1).

Synthesis of PVP Functionalized Gold Nanoparticles (PVP-b-AuNPs): 0.2 g solution of PVP was made in 100 mL of milli-Q water and allowed to stir at 80 °C for an hour. Aqueous PVP was added progressively to the AuNPs solution (100 mL). The hue went from dark brown to light brown after about an hour. After 10 min at room temperature, the product was centrifuged for 0.25 h, cleaned with Milli-Q water and dried in an oven at 70 °C for around two hours (Fig. 1).

Antimicrobial Activity: Gram-positive and Gram-negative bacterial strains were used to evaluate the biological properties of b-AuNPs and PVP-functionalized b-AuNPs utilizing a 96-well plate micro dilution approach[2]. Resazurin is used as a reference during the experiment. In summary, 50 µl of broth medium was added to each well of 96-well clear plates with a fat bottom in order to conduct microdilution susceptibility testing. To achieve concentration ranges of 0.254−5000 µg/mL, the test materials (100 µl) were serially diluted in broth medium in each matched well of a 96-well microtitre plate.

Fifty microliters of the working inoculum solution were added to each selected well to provide a final inoculum of 0.5–2.5× 105 CFU/ml. Internal controls, media only (media control), media with bacterial inoculum (bacterial growth control) and media with water (solvent controls) were all included in each test. The plates were then incubated at 37 °C for 20 hours. After 20 hours, 30 µl of resazurin was added to each well. The plate was then incubated for 30 minutes and the MIC was determined by recording the color change that was seen.

DPPH Assay: The DPPH technique was used to determine the antioxidant activity of both PVP-b-AuNPs and synthetic b-AuNPs[17]. During the experiment 20–120 µg/mL of ascorbic acid solution was considered as reference. A methanolic DPPH solution was used to assess the antioxidants.

Fig. 1: A Plant Leaves B Plant Extract C Synthesized b-AuNPs D Synthesized PVP-b-AuNPs

After combining 1 mL of the sample (20–120 µg/mL) with 1 mL of the DPPH solution, the experiment was allowed to sit at room temperature (25 °C) for 0.5 hours. A spectrophotometer was used to detect absorbance at a wavelength of 517 nm. The scavenging activity was determined as:

$$\text{Scavenging effect (\%)} = 1 - (A_{sample} / A_{control}) \times 100$$

Superoxide Anion Radical Scavenging Assay: As previously reported, the scavenging activity of superoxide anion radicals was determined[17]. Through interaction with superoxide radicals generated by the phenazinemethosulphate (PMS) and nicotinamide adenine dinucleotide (NADH) system, the purple formazan produced by nitro blue tetrazolium (NBT) was quantified using spectrophotometry. The absorbance at 560 nm was measured following five minutes of incubation at 25 °C in a reaction mixture including 1 mM NBT, 0.1 mM PMS, 1 mM NADH and different doses of b-AuNPs and PVP-b-AuNPs. Through comparison with the control group, the percentage of inhibition was determined. It was determined that the scavenging ability was:

$$\text{Scavenging effect (\%)} = [(Ac - As) / Ac] \times 100$$

Hydroxyl Radical Scavenging Assay: The decrease of ^{o}OH (hydroxyl radical) by peroxidation was used to quantify the hydroxyl radical scavenging activity. The relative stability of the materials (leaf extract, b-AuNPs and PVP-b-AuNPs) was also estimated[18]. 0.4 ml of 5.6 mM 2-deoxy-D-ribose in 50 mM KH_2PO_4–NaOH buffer (pH 7.4), 0.2 ml of 100 mM $FeCl_3$ and 104 mM of ethylene diamine tetraacetic acid (EDTA) (1:1 v/v) were combined with the 20–120 µg/ml solutions of b-AuNPs and PVP-b-AuNPs. The mixture was stirred and then incubated for 30 min at 50 °C. Following that, one milliliter of each of the 2.8% and 1% concentrations of TCA and TBA were added to each tube bearing the mixture. The sample was mixed and then heated to 50 °C for 30 min. Without a sample, the reaction mixture was seen at a wavelength of 532 nm. The identical formula used to generate the DPPH assay results was also used to obtain the hydroxyl radical scavenging assay results.

Hydrogen Peroxide Scavenging Assay: Despite a few minor adjustments, a technique akin to that of Makvana et al[18] was used to assess the removal of H_2O_2 by b-AuNPs and PVP-b-AuNPs. The mixture was incubated for 10 min at room temperature after being mixed with 2.4 ml of 0.1 M phosphate buffer (pH=7.4), b-AuNPs, PVP-b-AuNPs (20–120 µg/mL), BHT and 0.6 ml of 40 mM H_2O_2 solution. The hydrogen peroxide content was measured at 230 nm in relation to a phosphate buffer blank solution. The same formula used for the DPPH experiment was used to determine the H_2O_2 scavenging capability.

Reducing Power Measurement and Total Antioxidant Assay: To measure the reduction power, the previously described approach was used[20]. After preparing solutions of b-AuNPs and PVP-b-AuNPs (20–120 µg/mL), 0.1 mL of the sample solution, 0.2 M sodium phosphate buffer (pH = 6.6) and 1% $K_3[Fe(CN)_6]$ were combined. After incubating at 50 °C for 20 minutes, the mixture was chilled. Following the incubation period, trichloroacetic acid (10%w/v) was added. The mixture was then centrifuged for 10 minutes at 3000 rpm. After adding 0.10% ferric chloride, the absorbance of the supernatant was measured using spectrophotometry at a wavelength of 700 nm. BHT was used as a positive control.

A clear sign of the lowering activity was an increase in the solution's absorbance. Total antioxidant assay was calculated by applying the modified method. 3 ml solution including 28 mM sodium phosphate, 4 mM ammonium molybdate and 0.6 M sulfuric acid were combined with 20–120 µg/mL b-AuNPs and PVP-b-AuNPs. After that, the reaction mixture was allowed to incubate for 90 minutes at 95 °C before being cooled. The antioxidant experiment's findings were calculated using solution absorbance at 695 nm.

Results and Discussion

Characterization of b-AuNPs and PVP-b-AuNPs

UV–visible Spectroscopy: The aqueous reduction mixture was subjected to UV-visible spectroscopy to confirm the formation of b-AuNPs and PVP-b-AuNPs synthesized using *S. samarangense* leaf extract. Reduction of Au+3 to Au0 observed by color from pale yellow to reddish-brown, indicates the reduction of gold ions to gold nanoparticles, a process associated with surface plasmon resonance (SPR) characteristic of metal nanoparticles like gold[22]. The UV-visible spectrum of the b-AuNPs exhibited a prominent absorption peak at 535 nm (Fig. 2), corresponding to the SPR band of gold nanoparticles, confirming the successful synthesis of b-AuNPs with a size distribution supporting SPR activity. Similar results were also obtained by several researchers during their lab experiment[23-25].

Further analysis of PVP-functionalized b-AuNPs revealed a new absorption band between 520 and 550 nm (Fig. 2), indicating successful attachment of PVP to the b-AuNPs and a subsequent alteration of their optical properties, as evidenced by the broadening and slight red shift of the SPR peak. This shift is consistent with changes in the local refractive index due to PVP coating, similar to observations in other studies involving polymer-functionalized nanoparticles[26,27].

The *S. samarangense* leaf extract played a dual role in the synthesis process, acting as both a reducing agent for the gold ions and a stabilizing agent that capped the nanoparticles, preventing agglomeration. This dual function was crucial for maintaining the stability of the nanoparticles in solution, as indicated by the absence of significant spectral shifts that would suggest aggregation[28-30]. The observed SPR peak at 540 nm for b-AuNPs and the new absorption band for PVP-b-AuNPs are consistent with the findings in the

literature on plant extract-synthesized gold nanoparticles and polymer-functionalized nanoparticles respectively, underscoring the reliability of the experimental results[27,29]. Moreover, the functionalization with PVP enhanced the colloidal stability of the nanoparticles by providing a steric barrier, preventing agglomeration, a feature essential for applications in fields requiring long-term stability[13].

Fourier Transform Infrared Spectroscopy: The FTIR spectroscopy analysis of b-AuNPs and PVP-b-AuNPs synthesized using *S. samarangense* leaf extract provides valuable insights into the functional groups involved in nanoparticle synthesis and stabilization. The FTIR spectrum of the *S. samarangense* leaf extract displayed characteristic peaks at approximately 1058 cm^{-1}, 1384 cm^{-1} and 1626 cm^{-1}, corresponding to C–O stretching, C–H bending and C=O stretching vibrations respectively, indicating the presence of alcohols, phenols and carbonyl compounds essential for reducing gold ions and stabilizing the nanoparticles (Fig. 3).

In the FTIR spectrum of the biosynthesized b-AuNPs, significant shifts were noted at 3267 cm^{-1}, 2930 cm^{-1} and 1640 cm^{-1}, with the broad peak at 3267 cm^{-1} linked to O–H stretching vibrations, suggesting hydroxyl groups' involvement in reducing gold ions. The peak at 1640 cm^{-1} attributed to C=O stretching, hints at M–C=O formation during synthesis, highlighting the interaction between gold nanoparticles and organic molecules from the leaf extract[27,35]. The consistent peak at 1390 cm^{-1} across the leaf extract and b-AuNPs suggests the preservation of certain functional groups, such as C–H bonding, even after synthesis[22]. Upon PVP functionalization, additional peaks at 1760 cm^{-1} and 2950 cm^{-1} corresponding to the carbonyl (C=O) stretching of esters and C–H stretching vibrations of CH/CH_2 groups respectively were observed.

The 3290 cm^{-1} peak, associated with O–H stretching, indicates hydroxyl groups from PVP, which enhance nanoparticle stability by providing a steric barrier against agglomeration. These observations align with literature reports on PVP's role in stabilizing metal nanoparticles[28-30]. The FTIR analysis confirms that *S. samarangense* leaf extract serves both as reducing and capping agent, while PVP functionalization further stabilizes the b-AuNPs, supporting their suitability for various applications.

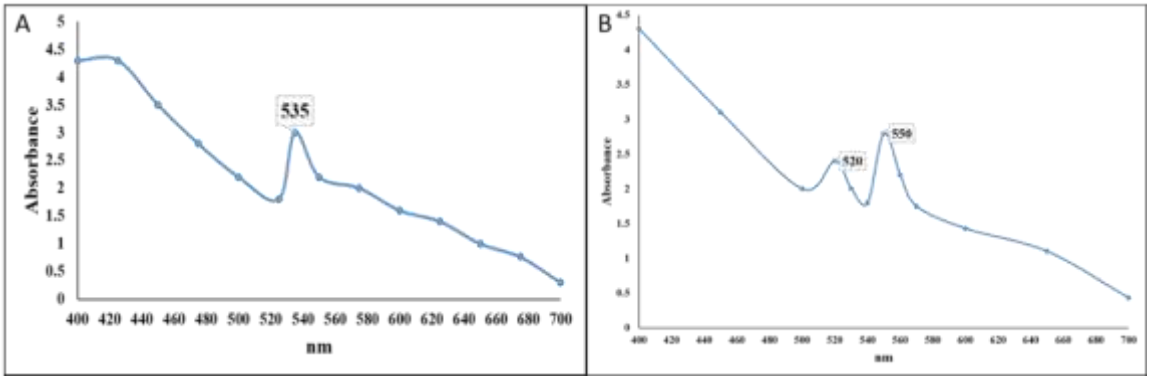

Fig. 2: UV–visible spectrum Analysis of (A) Synthesized b-AuNPs (b) Synthesized PVP-b-AuNPs

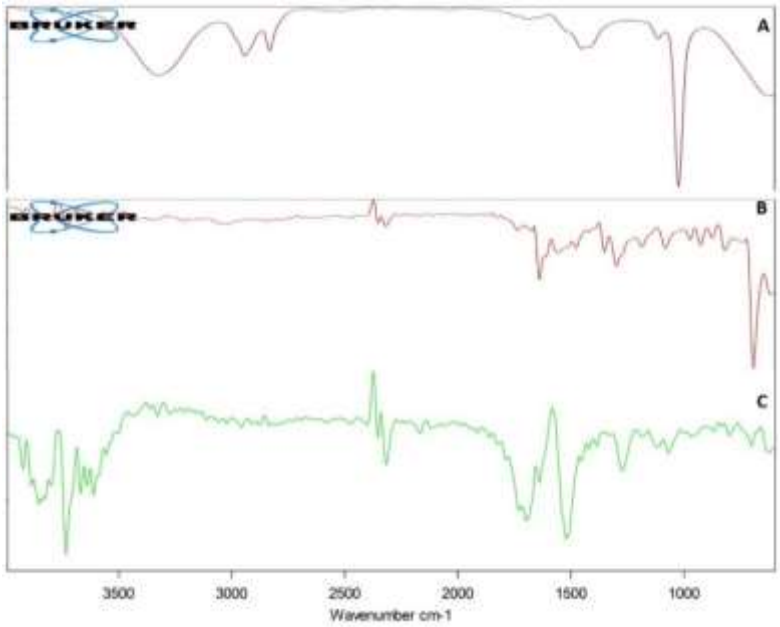

Fig. 3: FT-IR spectrum (A) *S. Samarangense* plant extract (B) b-AuNPs (C) PVP-b-AUNPs

X- Ray Diffraction: The XRD analysis of both b-AuNPs and PVP-b-AuNPs exhibit XRD patterns with distinct peaks corresponding to the FCC structure of gold, with key diffraction peaks observed at 38.20° (111), 44.28° (200), 64.47° (220), 77.42° (311) and 81.52° (222) (Fig. 4). These peaks match the standard gold diffraction pattern from the Joint Committee on Powder Diffraction Standards file no. 04-0784, indicating the successful synthesis of crystalline gold nanoparticles[2]4,28. The prominent (111) reflection highlights the preferential orientation of the nanoparticles, a common trait in XRD patterns of metallic nanoparticles, confirming their nano crystalline nature. The sharpness of these peaks suggests a narrow size distribution of the nanoparticles, with no significant broadening observed[22]. XRD pattern of PVP-b-AuNPs showed similar peaks, but with slight broadening and reduced peak intensity.

Particularly at the (111) and (200) planes, this broadening is attributed to a reduced crystallite size and the impact of the PVP coating might induce lattice distortions or strain[27]. The average crystallite size calculated using the Debye-Scherrer equation was approximately 10-15 nm for b-AuNPs, consistent with values reported for gold nanoparticles synthesized with plant extracts[23]. For PVP-b-AuNPs, the average size was slightly reduced to around 8-12 nm, indicating that PVP functionalization not only stabilizes the nanoparticles but also influences their growth and crystallization[24].

The XRD patterns showed no additional peaks, confirming the purity of the nanoparticles[30]. Comparison with HR-TEM and Selected Area Electron Diffraction results validated the crystallite size estimation and structural analysis[26]. The *S. samarangense* leaf extract contributes significantly to the reduction and stabilization of gold ions and the presence of phytochemicals in the extract directs the crystalline growth, as evidenced by the preferential orientation observed[13]. PVP functionalization further enhances the stability of the nanoparticles by preventing agglomeration and maintaining the FCC structure[23,24].

Overall, the XRD results confirm the formation of highly crystalline bimetallic gold nanoparticles with an average size of 8-15 nm, demonstrating the efficacy of the leaf extract and PVP in producing stable and well-defined nanoparticles suitable for diverse applications in catalysis, biomedicine and environmental remediation[22].

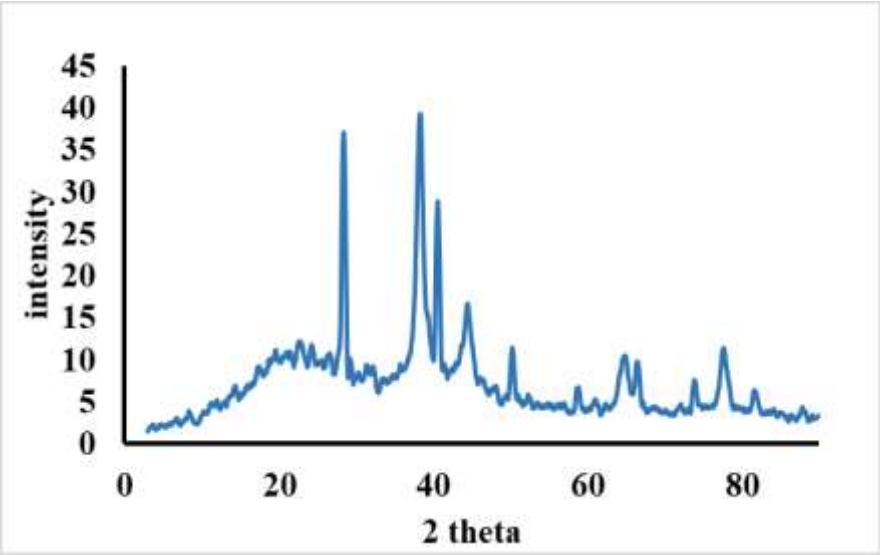

Fig. 4: XRD pattern of PVP-b-AuNPs

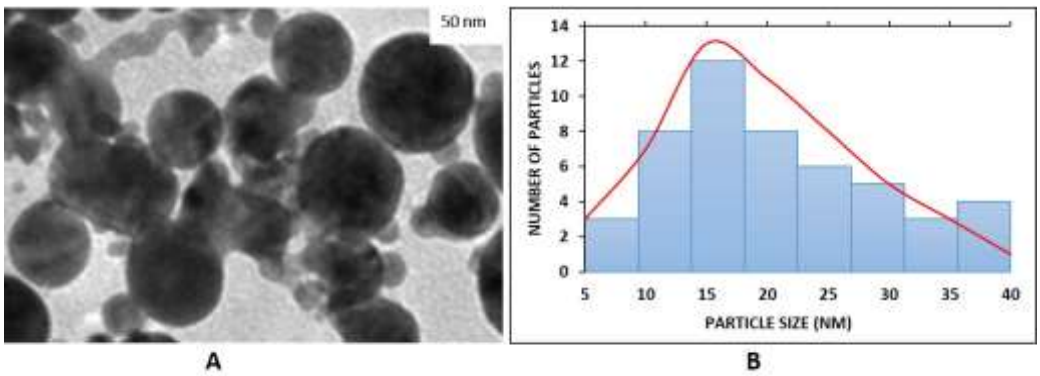

Fig. 5: (A) HR-TEM image of PVP-b-AuNPs observed at 50nm (B) Size distribution curve determined from TEM analysis and SAED pattern of PVP-functionalized b-AuNPs

HR-TEM Analysis: The HR-TEM analysis provides detailed insights into the size, morphology and dispersion of the b-AuNPs and PVP-b-AuNPs synthesized using *S. samarangense* leaf extract. HR-TEM images of both b-AuNPs and PVP-b-AuNPs reveal uniformly spherical (Fig. 5) well-dispersed particles with a high degree of homogeneity, confirming the successful synthesis of nanoparticles with controlled morphology[16]. The size of the biosynthesized b-AuNPs, as determined from HR-TEM images, was found to range between 10-15 nm, aligning well with the size estimates obtained from XRD analysis. Similarly, the PVP-b-AuNPs exhibited a slightly smaller size range of 8-12 nm, which is consistent with the XRD results and reflects the influence of PVP coating on nanoparticle size reduction and stabilization[19].

SAED patterns obtained from the HR-TEM analysis further corroborate the crystalline nature of the nanoparticles, displaying distinct ring patterns that correspond to the FCC structure of gold. The SAED results are in excellent agreement with the XRD data, indicating a consistent particle size range and crystalline phase[25,29]. The average size derived from SAED was approximately 4.62 ± 0.97 nm, slightly lower than the size observed in HR-TEM images which may be attributed to the influence of specific phytochemicals present in the *S. samarangense* leaf extract that affect nanoparticle growth and stabilizatio[13]. Hence, HR-TEM analysis confirms the successful synthesis of highly crystalline, spherical b-AuNPs and PVP-b-AuNPs with controlled size and morphology, supporting their potential application in various fields such as catalysis, biomedicine and environmental remediation[12,13].

Antimicrobial Assay of b-AuNPs and PVP-b-AuNPs: The antimicrobial assay results for b-AuNPs and PVP-b-AuNPs synthesized using *S. samarangense* leaf extract demonstrate their significant antibacterial activity against various bacterial strains. The assay was conducted using a resazurin-based 96-well plate micro dilution method, which allowed for the determination of the MIC and MBC of the nanoparticles against two Gram-negative bacteria, *E. coli* and *P. aeruginosa* and one Gram-positive bacterium, *S. aureus*[16]. The MIC values indicated that both b-AuNPs and PVP-b-AuNPs exhibited potent antibacterial activity, with PVP-b-AuNPs showing enhanced efficacy compared to b-AuNPs alone. The observed MIC values for PVP-b-AuNPs were notably lower, particularly against *S. aureus*, where they demonstrated superior inhibitory effects (Table 1).

This enhanced antibacterial activity of PVP-b-AuNPs can be attributed to the synergistic effects of the PVP coating and the bimetallic core, which may induce conformational changes in bacterial cell membranes, leading to increased membrane permeability and subsequent bacterial cell death[22]. The antimicrobial efficacy of PVP-b-AuNPs is likely to be influenced by the unique interaction between the nanoparticles and the bacterial cell walls, resulting in more effective disruption of cellular processes. Also, the MBC results further confirmed the bactericidal nature of the synthesized nanoparticles, with PVP-b-AuNPs exhibiting lower MBC values across all tested strains, indicating their strong bactericidal potential at lower concentrations.

The incorporation of PVP likely enhances the stability and dispersion of the nanoparticles, contributing to their increased interaction with bacterial cells and subsequent antimicrobial effects[18]. These findings are consistent with existing literature, which suggests that bimetallic nanoparticles, particularly those functionalized with polymers like PVP, exhibit superior antimicrobial properties due to their enhanced stability, improved bioavailability and increased interaction with microbial cell membranes[12]. The promising results from this study support further exploration of these nanoparticles for potential applications in antimicrobial therapies, particularly in the treatment of infections caused by both Gram-positive and Gram-negative bacteria.

Table 1
Plate determination of MIC and MBC of given sample

Sample	Raw	2	3	4	5	6	7	8	9	10	11	Tested Bacteria
	µg/ml	0.125	0.375	1.125	3.375	10.125	30.375	91.125	273.375	820.125	2460.375	
PVP-b-AuNPs	A	−	−	−	−	+	+	+	+	+	+	*E. coli*
b-AuNPs	B	−	−	−	+	+	+	+	+	+	+	*E. coli*
PVP	C	−	−	−	−	−	+	+	+	+	+	*E. coli*
b-AuNPs	D	−	−	−	+	+	+	+	+	+	+	*S. aureus*
PVP-b-AuNPs	E	−	−	−	−	−	+	+	+	+	+	*S. aureus*
PVP	F	−	−	−	−	−	−	+	+	+	+	*S. aureus*
b-AuNPs	G	−	−	−	+	+	+	+	+	+	+	*P. aeruginosa*
PVP-b-AuNPs	H	−	−	−	−	+	+	+	+	+	+	*P. aeruginosa*
PVP	I	−	−	−	−	−	+	+	+	+	+	*P. aeruginosa*

+, indicates bacterial growth inhibition; −, indicates no bacterial growth inhibition.

Antioxidant Properties of b-AuNPs and PVP-b-AuNPs: The antioxidant properties of b-AuNPs and PVP-b-AuNPs synthesized using *S. samarangense* leaf extract were evaluated using various assays including DPPH radical scavenging, superoxide radical scavenging, hydroxyl radical scavenging, hydrogen peroxide scavenging, reducing power measurement and total antioxidant capacity. These assays provided a comprehensive understanding of the nanoparticles' ability to neutralize different types of ROS and their overall antioxidant potential.

DPPH Radical Scavenging Activity: The DPPH assay revealed that both b-AuNPs and PVP-b-AuNPs exhibited a concentration-dependent increase in antioxidant activity. At 120 µg/mL, PVP-b-AuNPs demonstrated a remarkable 65.51% scavenging activity which was comparable to the 60.40% activity of ascorbic acid, a standard antioxidant (Fig. 6a). The enhanced DPPH scavenging effect of PVP-b-AuNPs can be attributed to the synergistic effects of PVP functionalization and the inherent antioxidant properties of the bimetallic nanoparticles.

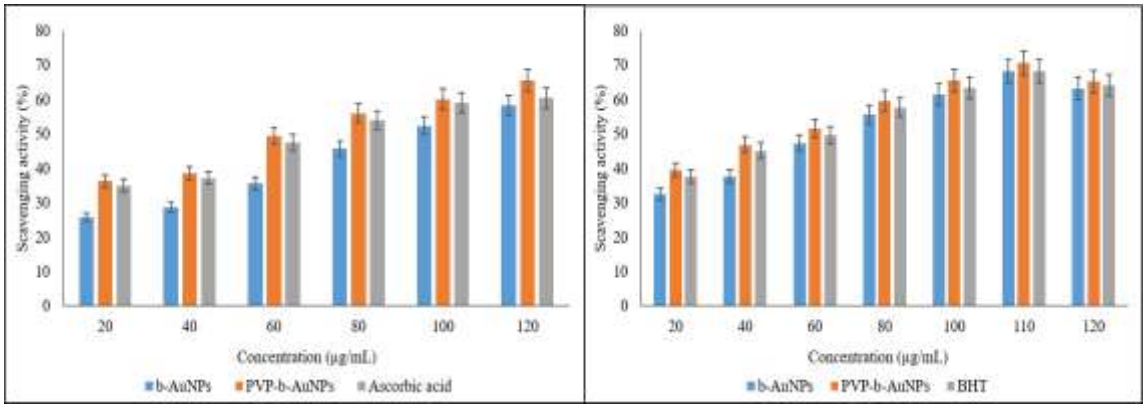

Fig. 6: (A) DPPH radical scavenging activity (B) Superoxide Radical Scavenging Activity

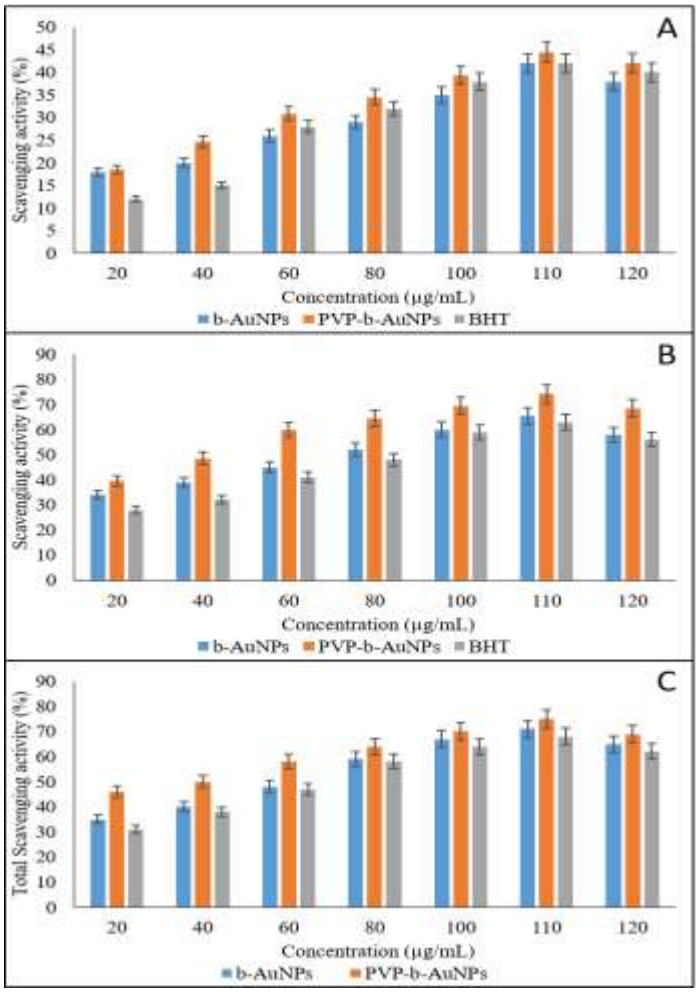

Fig. 7: (A) Hydroxyl Radical Scavenging Activity (B) Hydrogen Peroxide Scavenging Activity (C) Total Antioxidant Capacity

These findings suggest that PVP-b-AuNPs hold significant potential as effective free radical scavengers, offering a promising alternative or complement to conventional antioxidants[12,13,16].

Superoxide Radical Scavenging Activity: In the superoxide radical scavenging assay, PVP-b-AuNPs displayed superior scavenging activity with a 70.55% inhibition rate at 110 µg/mL, surpassing both b-AuNPs and the standard antioxidant, BHT, which exhibited a 68.23% inhibition rate (Fig. 6b). The higher scavenging ability of PVP-b-AuNPs is likely due to the enhanced interaction between the functionalized nanoparticles and superoxide radicals, leading to more effective neutralization of these reactive species. This enhanced activity underscores the potential of PVP-b-AuNPs as potent superoxide radical scavengers, which could be valuable in biomedical and therapeutic applications aimed at mitigating oxidative stress[13].

Hydroxyl Radical Scavenging Activity: The hydroxyl radical scavenging assay showed that both b-AuNPs and PVP-b-AuNPs were effective in intercepting hydroxyl radicals, with scavenging percentages of 42% and 44.53% respectively at 110 µg/Ml (Fig. 7a). These results highlight the nanoparticles' potential in suppressing lipid peroxidation, a critical process associated with oxidative damage and cellular injury. The slight superiority of PVP-b-AuNPs in hydroxyl radical scavenging further emphasizes their enhanced antioxidative properties[12].

Hydrogen Peroxide Scavenging Activity: The hydrogen peroxide scavenging activity was also significantly higher in PVP-b-AuNPs with a 74.20% inhibition rate compared to 65.40% for b-AuNPs and 62.91% for BHT (Fig. 7b). This high scavenging activity suggests that PVP-b-AuNPs are particularly effective in neutralizing hydrogen peroxide, a major ROS, thereby reducing the potential for oxidative stress and lipid peroxidation in biological systems[29].

Reducing Power and Total Antioxidant Capacity: The reducing power of PVP-b-AuNPs was found to be superior to that of b-AuNPs and BHT, indicating their strong electron-donating capacity which is essential for breaking the chain of free radicals. Additionally, the total antioxidant capacity assay showed that PVP-b-AuNPs exhibited the highest activity with a 75% total antioxidant capacity, surpassing both b-AuNPs and ascorbic acid (Fig. 7c). This superior antioxidant capacity reinforces the potential of PVP-b-AuNPs as effective agents in neutralizing oxidative stress[26]. The antioxidant assays demonstrate that PVP-b-AuNPs synthesized using *S. samarangense* leaf extract exhibit superior antioxidant properties across multiple assays compared to b-AuNPs and standard antioxidants like ascorbic acid and BHT.

The enhanced activity of PVP-b-AuNPs is attributed to the synergistic effects of PVP functionalization and the intrinsic properties of the bimetallic nanoparticles. These findings suggest that PVP-b-AuNPs have significant potential for biomedical applications, particularly in combating oxidative stress-related conditions.

Conclusion

This study successfully synthesized b-AuNPs and PVP-b-AuNPs using *S. samarangense* leaf extract. Characterization through UV-visible, FTIR, XRD and HR-TEM confirmed their morphological studies and formation with b-AuNPs showing peaks at 540 nm and PVP-b-AuNPs shifting to 520-550 nm. We have demonstrated antibacterial activity of PVP-b-AuNPs proving more effective and exhibited significant antioxidant properties. The results highlight the potential of these nanoparticles in biomedical and environmental applications.

Acknowledgement

All the authors kindly acknowledge the infrastructural support provided by Gokul Global University, Sidhpur. The experimental support from the Department of Chemsitry, Gokul Global University, Sidhpur and the HNGU, Patan, Guajrat, India is generously acknowledged.

References

1. Aktepe N. and Baran A., Green synthesis and antimicrobial effects of silver nanoparticles by pumpkin *Cucurbita maxima* fruit fiber, *Med. Sci*, **11**, 794-799 **(2022)**

2. Ali A., Emad N.A., Sultana N., Ali H., Jahan S., Aqil M., Mujeeb M. and Sultana Y., Medicinal potential of embelin and its nanoformulations: An update on the molecular mechanism and various applications, *Iranian Journal of Basic Medical Sciences*, **27(10)**, 1228 **(2024)**

3. Arodiya F., Makvana C. and Parmar K., Polymer Capped Silver Nanoparticles from *Ziziphus Nummularia* Leaves Extract: Potent Antibacterial and Antioxidant Activity, *Biosciences Biotechnology Research Asia*, **18(4)**, 691-701 **(2021)**

4. Basalius H., Mani A., Michael A., Mary S.M., Lenin M., Chelliah P., Siddiqui M.R., Wabaidur S.M. and Islam M.A., Green synthesis of nano-silver using *Syzygium samarangense* flower extract for multifaceted applications in biomedical and photocatalytic degradation of methylene blue, *Applied Nanoscience*, **13(6)**, 3735-3747 **(2023)**

5. Bukhari A., Ijaz I., Gilani E., Nazir A., Zain H., Saeed R., Alarfaji S.S., Hussain S., Aftab R. and Naseer Y., Green synthesis of metal and metal oxide nanoparticles using different plants' parts for antimicrobial activity and anticancer activity: a review article, *Coatings*, **11(11)**, 1374 **(2021)**

6. Das T., Kolli V., Karmakar S. and Sarkar N., Functionalisation of polyvinylpyrrolidone on gold nanoparticles enhances its anti-amyloidogenic propensity towards hen egg white lysozyme, *Biomedicines*, **5(2)**, 19 **(2017)**

7. Dlamini N.G., Basson A.K. and Pullabhotla V.S.R., Synthesis and characterization of various bimetallic nanoparticles and their application, *Applied Nano*, **4(1)**, 1-24 **(2023)**

8. Duman H., Akdaşçi E., Eker F., Bechelany M. and Karav S., Gold Nanoparticles: Multifunctional Properties, *Synthesis and Future Prospects*, **14(22)**, 1805 **(2024)**

9. Emetere M.E. and Ahiara I.M., Synthesis and characterization of aluminium coated Syzygium Samarangense extracts, *Chemical Data Collections*, **28**, 100418 **(2020)**

10. Fatima Z., Saleem R., Khan R.R.M., Liaqat M., Pervaiz M., Saeed Z., Muhammad G., Amin M. and Rasheed S., Green Synthesis, Properties and Biomedical Potential of Gold Nanoparticles: A Comprehensive Review, *Biocatalysis and Agricultural Biotechnology*, **59**, 103271 **(2024)**

11. Hamelian M., Varmira K. and Veisi H., Green synthesis and characterizations of gold nanoparticles using Thyme and survey cytotoxic effect, antibacterial and antioxidant potential, *Journal of Photochemistry and Photobiology B: Biology*, **184**, 71-79 **(2018)**

12. Iravani S. and Zolfaghari B., Green synthesis of silver nanoparticles using Pinus eldarica bark extract, *BioMed Research International*, **2013(1)**, 639725 **(2013)**

13. Jeetkar T.J., Khataokar S.P., Indurkar A.R., Pandit A. and Nimbalkar M.S., A review on plant-mediated synthesis of metallic nanoparticles and their applications, *Advances in Natural Sciences: Nanoscience and Nanotechnology*, **13(3)**, 033004 **(2022)**

14. Khan F., Shariq M., Asif M., Siddiqui M.A., Malan P. and Ahmad F., Green Nanotechnology: Plant-Mediated Nanoparticle Synthesis and Application, *Nanomaterials*, **12**, 673 **(2022)**

15. Kumar V. and Yadav S.K., Characterisation of gold nanoparticles synthesised by leaf and seed extract of *Syzygium cumini* L., *Journal of Experimental Nanoscience*, **7(4)**, 440-451 **(2012)**

16. Link S. and El-Sayed M.A., Shape and size dependence of radiative, non-radiative and photothermal properties of gold nanocrystals, *International Reviews in Physical Chemistry*, **19(3)**, 409-453 **(2000)**

17. Makvana C., Arodiya F. and Parmar K., Green synthesis of polymer-capped copper nanoparticles using Ocimum sanctum leaf extract: antibacterial and antioxidant potential, *Biosci. Biotechnol. Res. Commun*, **14**, 1832-1838 **(2021)**

18. Makvana C., Arodiya F., Limbachiya P. and Parmar K., Polymer Functionalization, Synthesis, Characterization and Biological Evaluation of Silver Nanoparticles Using Cucurbita Maxima Leaf Extract, Proceedings of the National Academy of Sciences, India Section B: Biological Sciences, 1-10 **(2024)**

19. Malik A.Q., Mir T.U.G., Kumar D., Mir I.A., Rashid A., Ayoub M. and Shukla S., A review on the green synthesis of nanoparticles, their biological applications and photocatalytic efficiency against environmental toxins, *Environmental Science and Pollution Research*, **30(27)**, 69796-69823 **(2023)**

20. Mittal A.K., Chisti Y. and Banerjee U.C., Synthesis of metallic nanoparticles using plant extracts, *Biotechnology Advances*, **31(2)**, 346-356 **(2013)**

21. Njeru Elosy Gatakaa, Kamweru Paul Kuria and Gichumbi Joel Mwangi, Natural dyes (Tithonia diversifolia, Tagetes minuta and Bidens pilosa) sensitized solar cells with reduced graphene based electrodes, *Res. J. Chem. Environ*., **28(10)**, 73-87 **(2024)**

22. Pourmadadi M., Shamsabadipour A., Aslani A., Eshaghi M.M., Rahdar A. and Pandey S., Development of polyvinylpyrrolidone-based nanomaterials for biosensors applications: a review, *Inorganic Chemistry Communications*, **152**, 110714 **(2023)**

23. Rai M., Ingle A.P., Birla S., Yadav A. and Santos C.A.D., Strategic role of selected noble metal nanoparticles in medicine, *Critical Reviews in Microbiology*, **42(5)**, 696-719 **(2016)**

24. Raval S.Y., Arya P., Jain M., Sosa T., Trivedi P., Dabhi R. and Raval V.H., Sustainable biosynthesis of β-carotene utilizing sugarcane bagasse: depiction and biotechnological implications, *Biomass Conversion and Biorefinery*, **2024**, 1-16 **(2024)**

25. Rey-Méndez R., Rodríguez-Argüelles M.C. and González-Ballesteros N., Flower, stem and leaf extracts from *Hypericum perforatum* L. to synthesize gold nanoparticles: Effectiveness and antioxidant activity, *Surfaces and Interfaces*, **32**, 102181 **(2022)**

26. Sagadevan S., Fatimah I., Anita Lett J., Rahman M.Z., Leonard E. and Oh W.C., Eco-friendly green approach of nickel oxide nanoparticles for biomedical applications, *Open Chemistry*, **21(1)**, 20230141 **(2023)**

27. Singh P., Kim Y.J., Zhang D. and Yang D.C., Biological synthesis of nanoparticles from plants and microorganisms, *Trends in Biotechnology*, **34(7)**, 588-599 **(2016)**

28. Tarigan C., Pramastya H., Insanu M. and Fidrianny I., Syzygium samarangense: review of phytochemical compounds and pharmacological activities, *Biointerface Res. Appl. Chem*, **12(2)**, 2084-2107 **(2022)**

29. Thi Q.V., Tamboli M.S., Ta Q.T.H., Kolekar G.B. and Sohn D., A nanostructured MOF/reduced graphene oxide hybrid for enhanced photocatalytic efficiency under solar light, *Materials Science and Engineering: B*, **261**, 114678 **(2020)**

30. Yulizar Y., Ariyanta H.A. and Abduracman L., Green synthesis of gold nanoparticles using aqueous garlic (*Allium sativum* L.) Extract and its interaction study with melamine, *Bulletin of Chemical Reaction Engineering & Catalysis*, **12(2)**, 212-218 **(2017)**.

(Received 15th March 2025, accepted 21st April 2025)